

# Preparation of photoelectrode CNT/TiO<sub>2</sub> doped ZnO nanocomposite by sol-gel method for dye-sensitized solar cell

MOHD ZIKRI RAZALI<sup>a</sup>, HUDA ABDULLAH<sup>\*a</sup>, SAHBUDIN SHAARI<sup>b</sup>, MOHD RAIHAN TAHA<sup>c</sup>

<sup>a</sup>*Department of Electrical, Electronic & System, Faculty of Engineering and Built Environment, Universiti Kebangsaan Malaysia, 43600 Bangi, Selangor, Malaysia*

<sup>b</sup>*Institute of Microengineering and Nanoelectronics (IMEN), Universiti Kebangsaan Malaysia, 43600 Bangi, Selangor, Malaysia*

<sup>c</sup>*Department of Civil and Structural Engineering, Faculty of Engineering and Built Environment, Universiti Kebangsaan Malaysia, 43600 Bangi, Selangor, Malaysia*

This study aims to get unique morphological structure of CNT/TiO<sub>2</sub> doped ZnO nanocomposite using sol-gel method for better DSSC efficiency. The ZnO solution was prepared as follows; zinc acetate was dissolved in ethanol and stirred for 15 min at 60 °C. The CNT/TiO<sub>2</sub> solution start with a combination of 2-propanol (50 ml) anhydrate, TTIP and 0.5 gram of CNT were initially prepared. The 2 solution were combined and stirred vigorously. All samples are designated as CNT/TiO<sub>2</sub> – x, where x is the mol % of the Zn [x = (a) 0.1, (b) 1.5 and (c) 2.5]. The SEM analysis images composed of porous TiO<sub>2</sub> and nanoflake ZnO nanocomposite, and the thickness of the CNT/TiO<sub>2</sub> doped ZnO paste sample is around 19.73 µm. The XRD analysis showed two different main peaks for TiO<sub>2</sub> (110) and ZnO (101) were formed as anatase/hexagonal structure. The crystalline size of anatase TiO<sub>2</sub> nanoparticle was 18.04 nm, and hexagonal ZnO were 40.99 nm and 73.78 nm in diameter. The percentages efficiency ( $\eta$ ) for 0.5 %, 1.5 % and 2.5 mol % were as follows 2.2 %, 2.4 % and 2.8 %, respectively.

(Received October 25, 2013; accepted May 15, 2014)

**Keywords:** CNT/TiO<sub>2</sub>, ZnO, Sol-gel method, Dye-sensitized solar cell (DSSC)

## 1. Introduction

Dye-sensitized solar cells (DSSC) are a brand-new type technology for changing light energy into electrical energy. It is composed of a dye-modified wide band semiconductor electrode such as TiO<sub>2</sub>, ZnO, Nb<sub>2</sub>O<sub>5</sub> and a counter electrode and redox electrolyte [1-2]. Because of its low fabrication cost, its robust nature, environmental compatibility, and the simplicity of the process, interest in DSSC has grown considerably. Although the cost of DSSC fabrication is cheaper compared to a silicon solar cell, for practical application an improved efficiency and long-term stability are needed [3-4].

In recent years, semiconductor photo-catalysis is becoming more and more attractive due to its great potential to solve environmental problems [5]. Titanium dioxide (TiO<sub>2</sub>) was one of the most important semiconductors with high photo-catalytic activity, being non-toxic, stable in aqueous solution, and relatively inexpensive. The excellent photo-catalytic property of TiO<sub>2</sub> is due to its wide-band gap and long lifetime of photo-generated holes and electrons. The material, however, presents two main drawbacks during the photo-catalytic process: (i) the low use of solar spectrum and (ii) the relatively high electron-hole recombination rate. One of the efforts to overcome these problems is to dope TiO<sub>2</sub>

with other material [6-7]. As another well-known photo-catalyst, the zinc oxide (ZnO) material has received much attention with respect to the degradations of various environmental pollutants. In fact, higher photo-catalytic efficiency, compared to TiO<sub>2</sub>, has been reported for ZnO [8]. Besides, the band gap energy of ZnO was similar to that of TiO<sub>2</sub> (approximately 3.2 eV) [9]. Thus, it is possible to enhance the activity of TiO<sub>2</sub> photo-catalyst by ZnO doping. Up to now, some efforts have been done to modify TiO<sub>2</sub> by ZnO doping. The physical, chemical, and photochemical properties of the formed TiO<sub>2</sub>/ZnO composites were mainly dependent on the manufacturing method. For instance, other researchers synthesised TiO<sub>2</sub>/ZnO nanopowder by the hydrothermal method. Other inventors prepared Zn-doped TiO<sub>2</sub> film by pulsed DC reactive magnetron sputtering method using Ti and Zn mixed target and production ZnO coated TiO<sub>2</sub> nanoparticles for use in flexible dye-sensitized solar cells [10-11]. Contrary to these materials, the TiO<sub>2</sub>/ZnO nanocomposite film via sol-gel process has advantages of higher surface activity due to the nanoparticles, being not conglomerated and smoothly reclaimed after reaction. Moreover, the sol-gel process for nano film preparation, compared to other methods, has notable advantages such as high purity, good uniformity of the film nanostructure and freely controlled reaction condition [12].

The aims and objectives of this study are to synthesize CNT/TiO<sub>2</sub> doped ZnO solution, fabricate dye sensitised solar cell and analyze the morphology and structural design of the thin film. The motivation of this study is to get better solar cell percentage efficiency with combination of CNT/TiO<sub>2</sub> and ZnO nanocomposite.

## 2. Methodology

### ZnO solution

The preparation of CNT/TiO<sub>2</sub> doped ZnO sol-gel could be obtained via directly mixing of the acidic TiO<sub>2</sub> and the ZnO solution. The ZnO solution was prepared as follows. At first, zinc acetate (R&M Chemicals, 99.5 %) at different mol % – (a) 0.5 %, (b) 1.5 % and (c) 2.5 % was dissolved in ethanol and stirred for 15 min at 60 °C on a hot plate to get a precursor solution. A mixture of distilled water, diethanolamine, and ethanol was then dropped into the precursor solution with vigorous stirring. Then, the solution was continuously stirred for 1 h to achieve a transparent alkaline ZnO solution. Fig. 1 shows the flow chart diagram for ZnO solution preparation method.

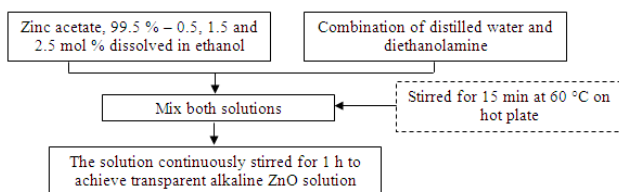


Fig. 1. Preparation of ZnO solution flow chart.

### CNT/TiO<sub>2</sub> doped ZnO solution

The sol-gel method with acid-catalysed modification used to prepare the CNT/TiO<sub>2</sub> nanocomposite. The combined solutions of 2-propanol (50 ml) anhydrate and 0.5 g of CNT were initially being prepared, with

sonication for about 30 min. The sonicated CNT/2-propanol solutions were then being introduced with a small amount of titanium tetraisopropoxide (TTIP) (Aldrich, 97 %) and directly stirring vigorously to enhance the interaction between the two substances for an additional 60 min. The CNT/TiO<sub>2</sub> solution combines with Carbowax 400 after cooling down to room temperature. Finally, the ZnO solution (0.5 %, 1.5 % and 2.5 mol %) and CNT/TiO<sub>2</sub> solutions were combined and stirred vigorously. Fig. 2 shows the flow chart diagram for CNT/TiO<sub>2</sub> doped ZnO solution preparation method.

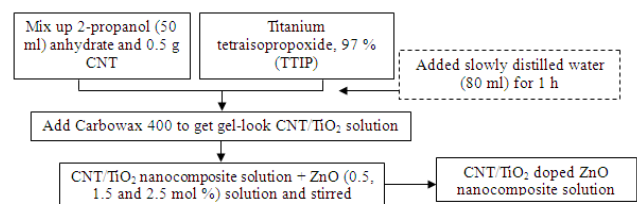


Fig. 2. Preparation of CNT/TiO<sub>2</sub>doped ZnO solution flow chart.

### Dye-sensitized solar cell fabrication

The CNT/TiO<sub>2</sub> doped ZnO thin films were doctor-bladed on the ITO glass substrates that formed 0.25 cm<sup>2</sup> active regions and annealed at 450 °C for 30 min. The thin films were then immersed in an absolute ethanol solution of ruthenium dye (N719, Solaronix) for one day. As for counter electrode, a platinum electrode was deposited on a conductive glass substrate by screen printing technique. A sandwich-type solar cell was assembled by clipping both electrode and counter electrode together and put some electrolyte solution. Iodolyte MPN-100 from Solaronix was used as electrolyte for this solar cell. Fabrication of dye-sensitized solar cell is completed. Fig. 3 shows the flow chart diagram for CNT/TiO<sub>2</sub> dye-sensitized solar cell preparation method.

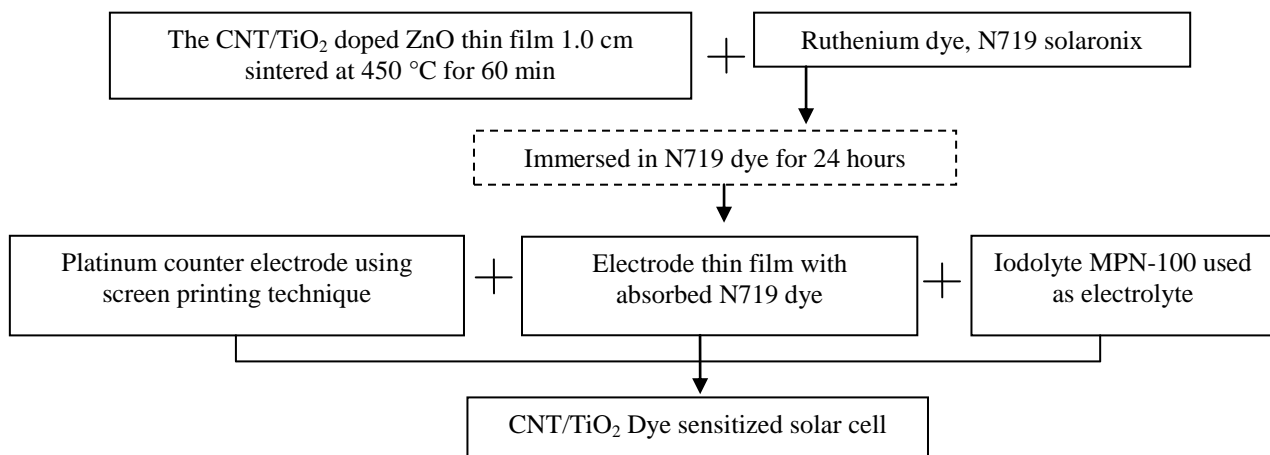


Fig. 3. Preparation of CNT/TiO<sub>2</sub>doped ZnO dye-sensitized solar cell flow chart.

### 3. Result and discussion

#### Field emission scanning electron micrograph (FESEM)

The field emission scanning electron micrograph (FESEM) images in Fig. 4 show morphological structure and EDX graph for CNT/TiO<sub>2</sub> thin films which were doped with different ZnO doping concentration. The thickness of the CNT/TiO<sub>2</sub> doped ZnO paste sample is around 19.73  $\mu\text{m}$ . The measurement range employed was 200 nm with a 50,000 $\times$  magnification. It can be seen that, the crystallites are spherical/flake nanoparticles, and the average diameter of CNT/TiO<sub>2</sub> doped ZnO (0.5, 1.5 and 2.5 mol %) is about 25-50 nm. The surface morphology of the CNT/TiO<sub>2</sub> doped ZnO shows that the structure is quite compact for practically all the three samples. The combination of CNT/TiO<sub>2</sub> nanocomposite doped ZnO with different mol %: 0.5 %, 1.5 % and 2.5 % forming a unique CNT/TiO<sub>2</sub> nanoparticle and ZnO nanoflakes structure [13].

After annealed at 450  $^{\circ}\text{C}$  for 30 min we can see nearly homogenous structure with no cracks appeared from the morphological structure and cross-section area. The thin films are also composed of high porosity pigment. This can help to ease the absorption of dye into the nanocomposite particles and hence can increase the photo conversion efficiency of the solar cell. EDX analysis shows that CNT/TiO<sub>2</sub> doped ZnO thin films composed of carbon, titanium, oxygen and zinc elements which are different according to the doping concentration.

Table 1 shows the EDX parameter data for carbon, titanium, oxygen and zinc elements. The titanium and carbon elements decreased in weight percentages with 53.19 %, 52.56 % and 51.82 % for titanium and 21.55 %, 20.98 % and 20.23 % for carbon, respectively. Zinc element as expected increase to 19.14 %, 23.11 % and 25.08 % with each doping concentration. Thus, with high surface area CNT/TiO<sub>2</sub> nanoparticles/nanoflake thin films doped ZnO are successfully synthesized [14].

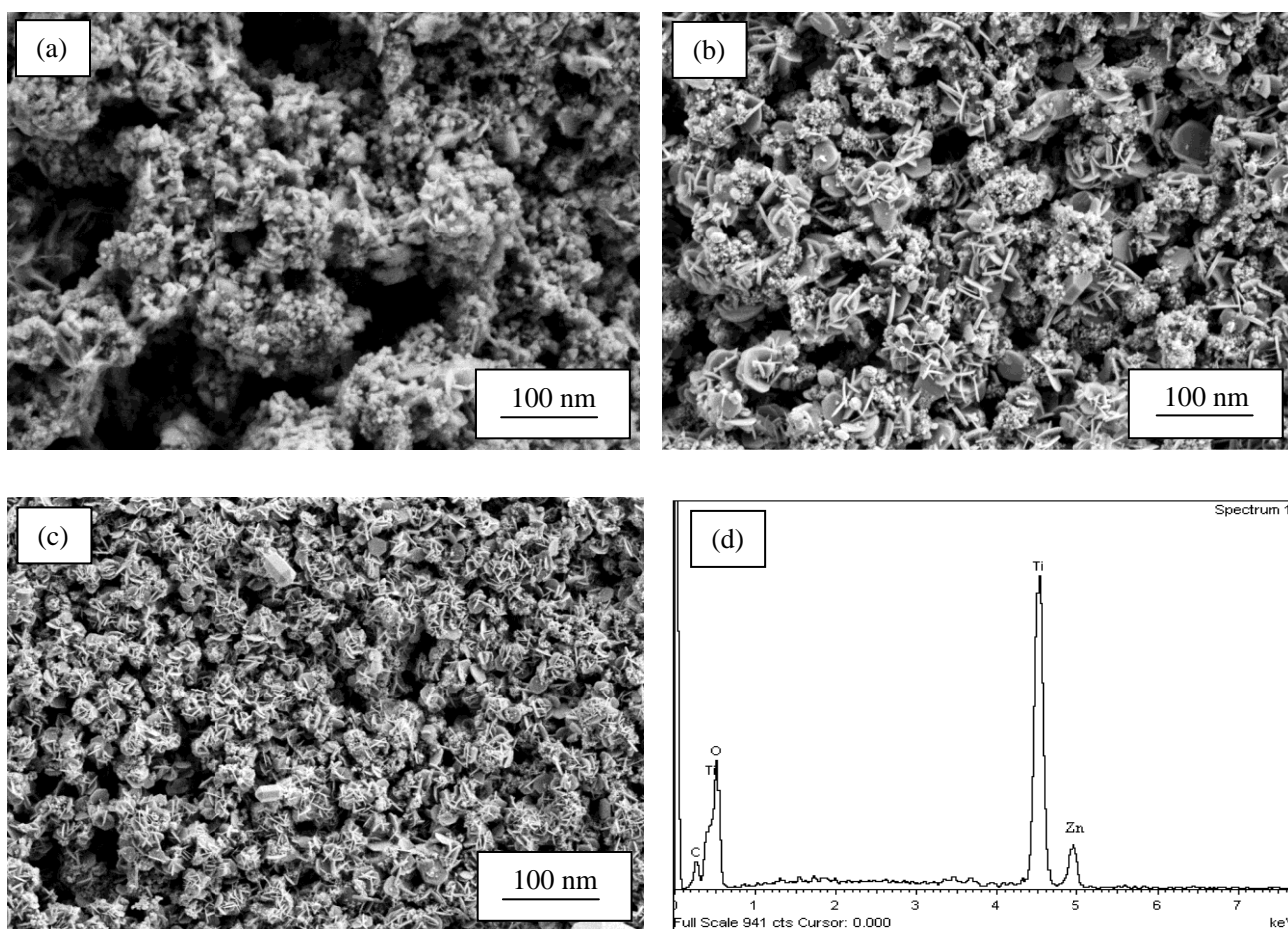


Fig. 4. FESEM images of CNT/TiO<sub>2</sub> doped ZnO for (a) 0.5 %, (b) 1.5 %, (c) 2.5 % thin film annealed at 450  $^{\circ}\text{C}$  and (d) EDX graph.

Table 1. EDX weight percentage analysis for sample CNT/TiO<sub>2</sub> doped ZnO.

Sample	Weight Percentage, %				
	ZnO, mol %	Oxygen (O)	Titanium (Ti)	carbon (C)	Zinc (Zn)
(a)	0.5	6.12	53.19	21.55	19.14
(b)	1.5	3.35	52.56	20.98	23.11
(c)	2.5	2.87	51.82	20.23	25.08

### X-ray diffraction (XRD)

X-ray diffraction (XRD) analysis has been conducted using x-ray diffractometer at diffraction angle of 20° – 60° theta. Fig. 5 shows the annealed thin film was identified as titanium dioxide (TiO<sub>2</sub>) by PDF No. JCP2.2CA: 01-086-1156 and PDF No. JCP2.2CA: 01-078-2486 reference and zinc oxide (ZnO) by PDF No. JCP2:01-089-1397 reference. The crystalline structure of the CNT/TiO<sub>2</sub> doped ZnO nanocomposite with the corresponding 2θ values and crystal planes are presented in Fig. 6 and Table 2. The apparent peaks at 2θ values of 31.68°, 34.40°, 36.20°, 47.52° and 56.52° correspond to the crystal planes of (100), (002), (101), (102) and (110) that conforming the present of ZnO. On the other hand, the values of 25.20°, 26.68°, 41.12° and 54.32° that correspond to the crystal planes of (101), (110), (111) and (211) showing the present of TiO<sub>2</sub>, which was found to be similar to that reported in literature [15].

The presence of major peak at 36.20° (2θ) with crystal plane (101) in hexagonal phase of ZnO and major peak at 26.68° (2θ) with crystal plane (110) in anatase phase of TiO<sub>2</sub> for this nanocomposite revealed that ZnO was well-doped on the surface of TiO<sub>2</sub> nanoparticle. Hexagonal structure of ZnO which was shown by strong peak between 30° and 40°(2θ) supported this experimental result [16]. The shifting of 2θ peaks from higher 26.68° (110) towards lower values 25.20° (101) of TiO<sub>2</sub> in this nanoparticle TiO<sub>2</sub> and nanoflake ZnO is an indication of the mixing of two oxides in crystalline level. This result confirms the incorporation of CNT/TiO<sub>2</sub> doped ZnO and simultaneously supports the FESEM and XRD analysis [17].

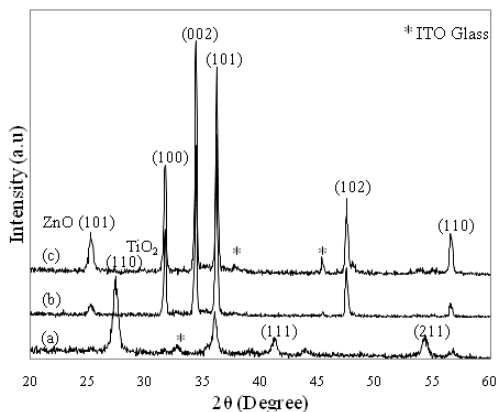


Fig. 5. XRD diffractograph of CNT/TiO<sub>2</sub> doped ZnO for (a) 0.5 %, (b) 1.5 % and (c) 2.5 % thin film annealed at 450 °C.

The average crystalline size of the particles was calculated from the XRD (101) ZnO peak hexagonal phase and (110) TiO<sub>2</sub> peak anatase phase by applying the Scherrer's formula [18-19].

$$D = \frac{k\lambda}{B \cos \theta} \quad (1)$$

From the equation above, the average crystalline size composes of Scherrer's constant (k), the X-ray wavelength (λ), the broadening of the diffraction line measured as the full width at half maximum intensity (FWHM) (B), the corresponding diffraction angle and the main peak position (θ). The crystallite size of anatase TiO<sub>2</sub> was found to be (a) 73.78 nm, and hexagonal ZnO were (b) 40.99 nm and (c) 18.04 nm in diameter when calcined at 450 °C and was indicated in Table 2. Fig. 6 shows that the crystalline sizes of the samples graphically. When the mol % of the zinc ion doping in TiO<sub>2</sub> was increased, the crystallite size decreased. The particle sizes in the samples are in the range of 10 – 80 nm [20].

Table 2. Calculation of crystallite size and major peak parameter for CNT/TiO<sub>2</sub> doped ZnO.

Sample	ZnO, mol %	Crystallite Size, nm	Major Peak
(a)	0.5	18.04	110
(b)	1.5	40.99	101
(c)	2.5	73.78	101

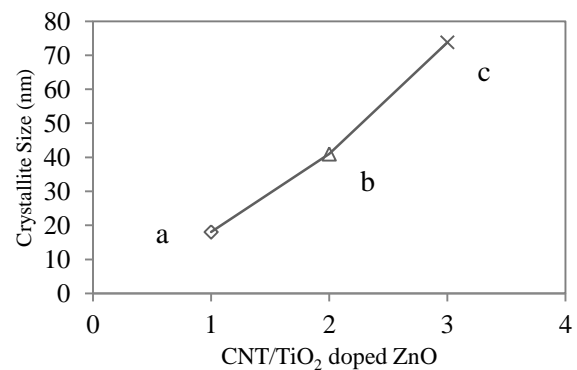


Fig. 6. Crystallite size graph versus samples for CNT/TiO<sub>2</sub> doped ZnO.

### Photovoltaic efficiency

Photovoltaic IV curve experiment has been performed using GAMRY INSTRUMENTS G300 using physical electrochemistry software under simulated AM 1.5G solar illumination using a 1000 Wm<sup>-2</sup> xenon lamp [21]. Fig. 7 shows the IV curve graph for CNT/TiO<sub>2</sub> doped ZnO dye-sensitized solar cell with doping concentration (a) 0.5 %, (b) 1.5 % and (c) 2.5 %. Table 3 illustrates the IV curve graph in terms of open-circuit voltage ( $V_{oc}$ ), short circuit current ( $J_{sc}$ ), fill factor (%) calculated from the maximum cell output power and the product ( $V_{oc} \times J_{sc}$ ) and percentage efficiency ( $\eta$ ) value. Fig. 8 shows the graphical data of CNT/TiO<sub>2</sub> doped ZnO. Different ZnO doping concentrations in CNT/TiO<sub>2</sub> influenced the photovoltaic performance; the high ZnO doping concentration - 2.5 % in CNT/TiO<sub>2</sub> DSSC gave the highest efficiency performance about 2.8 % with the  $V_{oc}$  of 0.65 V,  $J_{sc}$  of 7.12 mA.cm<sup>-2</sup> and fill factor of 60 %. The CNT/TiO<sub>2</sub> doped with 1.5 % ZnO gave the value of efficiency around 2.4 % with  $V_{oc}$  of 0.58 V,  $J_{sc}$  of 7.11 mA.cm<sup>-2</sup> and fill factor of 58 % followed with the least efficient CNT/TiO<sub>2</sub> doped 0.5 % ZnO with 2.2 % efficiency with  $V_{oc}$  of 0.59 V,  $J_{sc}$  of 6.78 mA.cm<sup>-2</sup> and fill factor of 55 % as you can see in Table 3.

The efficiency increase might be due to the changing in morphological structure of CNT/TiO<sub>2</sub> with different doping concentration of ZnO. This can be supported from the FESEM and XRD result that showed the nanostructure CNT/TiO<sub>2</sub> doped ZnO become bigger in crystalline size with addition of ZnO nanoparticles. Based on other researchers photovoltaic experimental results, the combination of TiO<sub>2</sub> and ZnO nanopowder will provide an inherent energy barrier that led to a decrease in recombination thus the value of  $J_{sc}$ ,  $V_{oc}$ , fill factor and overall conversion efficiency were increased from 0.35 mA.cm<sup>-2</sup> to 0.49 mA.cm<sup>-2</sup> for  $J_{sc}$ , from -0.67 V to -0.72 V for  $V_{oc}$ , from 61.1 % to 69.0 % for fill factor and 0.71 % to 1.21 % for overall conversion efficiency [22].

On the other hand, when the surface of porous TiO<sub>2</sub> nanoparticles thin film is covered by ultra-fine ZnO nanoparticles, it creates aggregates, which is formed by the N719 dye and Zn<sup>2+</sup> ions. These aggregates may obstruct the electron injection from the LUMO of N719 dye to the conduction band of ZnO and decrease the short-circuit photocurrent and performance of the DSSC [23]. Additionally, exposing ITO substrate to electrolyte enhances electron recombination of operating DSSC and can limit the DSSC performance [24].

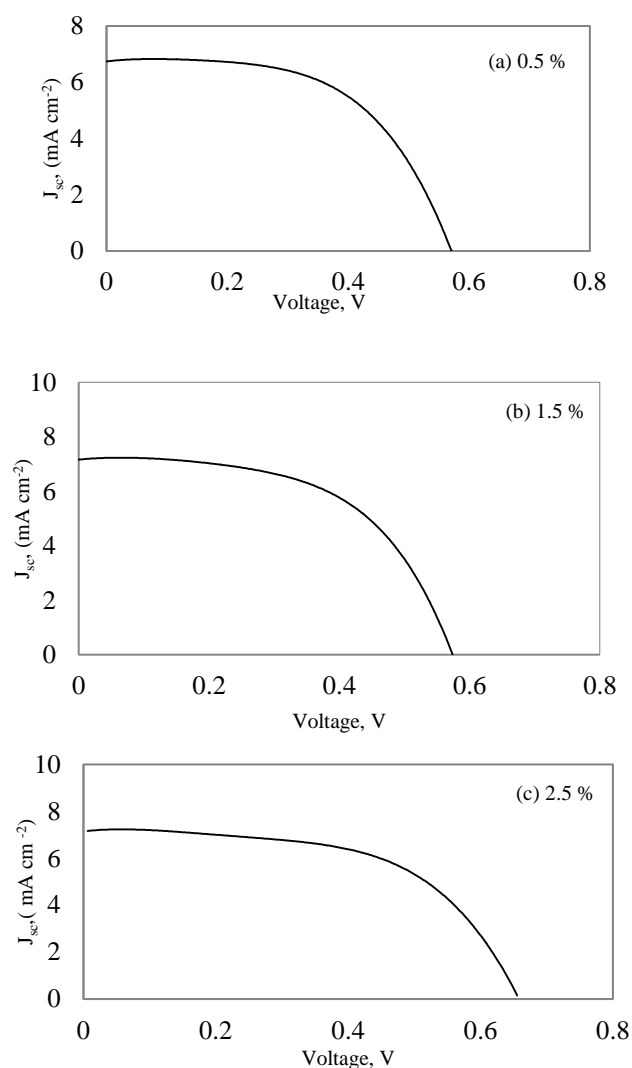


Fig.7. IV curve graph for CNT/TiO<sub>2</sub> doped ZnO dye-sensitized solar cell.

Table 3. Photovoltaic performance for CNT/TiO<sub>2</sub> doped ZnO dye-sensitized solar cell.

Sampl e	ZnO, mol %	$V_{oc}$ , V	$J_{sc}$ , mA.cm <sup>-2</sup>	Fill Factor, %	Efficiency, %
(a)	0.5	0.59	6.78	0.55	2.2
(b)	1.0	0.58	7.11	0.58	2.4
(c)	2.5	0.65	7.12	0.60	2.8

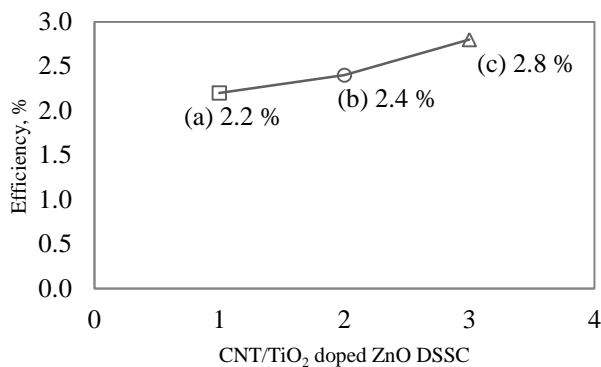


Fig. 8. Photovoltaic efficiency trend for CNT/TiO<sub>2</sub> doped ZnO dye-sensitized solar cell.

#### 4. Conclusion

In this study, the fabrication of CNT/TiO<sub>2</sub> doped ZnO nanocomposite films as a photoanode for dye-sensitized solar cell had been successfully prepared. These thin films are composed of homogeneously porous TiO<sub>2</sub> nanoparticles and ZnO nanoflake composite without cracks. The XRD analysis supported the FESEM analysis results with graphical data showing that ZnO is in hexagonal phase and TiO<sub>2</sub> is in anatase phase with major peaks for ZnO nanoflake (110) in crystal plane and for TiO<sub>2</sub> nanoparticles (101) plane. The crystallite size for all three samples becomes smaller with addition of ZnO in CNT/TiO<sub>2</sub> nanocomposite solution. The photovoltaic percentage efficiency for CNT/TiO<sub>2</sub> doped ZnO dye-sensitized solar cell is higher for 2.5 mol % ZnO doping with 2.8 % compared to other doped ZnO DSSC; with 2.2 % and 2.4 %. The high porosity and unique structural design of CNT/TiO<sub>2</sub> nanocomposite and ZnO nanoflake ease the electron transportation between the thin films nanoparticles covered with dyes. This phenomenon can enhance the dye-sensitized solar cell photovoltaic efficiency.

#### Acknowledgements

The author would like to thank the laboratory of photonics Institute of Microengineering and Nanoelectronic (IMEN), Universiti Kebangsaan Malaysia for providing the facilities.

#### References

- [1] Y. Shen, H. Deng, J. Fang, Z. Lu, *Colloids and Surfaces A: physicochemical and Engineering Aspects*, **175**, 135 (2000).
- [2] B. O'Regan, M. Grätzel, *Nature*, **353**, 737 (1991).
- [3] L. M. Peter, K. G. U. Wijayantha, *Electrochim. Acta.*, **45**, 4543 (2000).
- [4] S. Tanaka, *Jpn. J. Appl. Phys.*, **40**, 97 (2001).
- [5] L. Jing, B. Xin, F. Yuan, B. Wang, K. Shi, W. Cai, H. Fu, *Appl. Catal. A: Gen.*, **275**, 49 (2004).
- [6] X. Zhang, F. Zhang, K. Y. Chan, *Mater. Chem. Phys.*, **97**, 384 (2006).
- [7] P. Pichat, *Nouv. J. Chem.*, **11**, 135 (1987).
- [8] V. Houskova, V. Stengl, S. Bakardjieva, N. Murafa, A. Kalendova, F. Oplustil, *J. Phys. Chem. Solids*, **68**, 716 (2007).
- [9] D. K. Zhang, Y. C. Liu, Y. L. Liu, H. Yang, *Physica B*, **351**, 178 (2004).
- [10] W. Zhang, S. Zhu, Y. Li, F. Wang, *Vacuum*, **82**, 328 (2008).
- [11] S. S. Kim, J. H. Yum, Y. E. Sung, *J. Photochem. Photobiol. A: Chemistry*, **171**, 269 (2005).
- [12] P. Chrysicopoulou, D. Davazoglou, C. Trapalis, G. Kordas, *Thin Solid Films*, **323**, 188 (1998).
- [13] H. Abdullah, A. Omar, M. A. Yarmo, S. Shaari, M. R. Taha, *Journal of Materials Science: Materials in Electronics*, **24**(9), 3603 (2013).
- [14] A. Omar, H. Abdullah, S. Shaari, M. R. Taha, *J. Mater. Res.*, **28**(13), 1 (2013).
- [15] Y. Jiang, Y. Sun, H. Liu, F. Zhu, H. Yin, *Dyes Pigment*, **78**, 77 (2008).
- [16] N. P. Ariyanto, H. Abdullah, N. S. A. Ghani, *Mater. Res. Inno.*, **13**(3), (2009).
- [17] H. R. Pant, C. H. Park, B. Pant, L. D. Tijing, H. Y. Kim, *Ceramics International*, **38**, 2943 (2012).
- [18] B. D. Cullity, S. R. Stock, 3<sup>rd</sup> Ed, Prentice-Hall, 2001.
- [19] H. Abdullah, N. P. Ariyanto, S. Shaari, B. Yulianto, S. Junaidi, *American J. of Engineering and Applied Science* **2**, **1**, 236 (2009).
- [20] T. B. Nguyen, M. J. Hwang, K. S. Ryu, *Korean Chem. Soc.*, **33**, 1 (2012).
- [21] H. Abdullah, M. Z. Razali, S. Shaari, M. R. Taha, *Electronic Materials Letters*, DOI: 10.1007/s13391-013-3132-0.
- [22] S. S. Kim, J. H. Yum, Y. E. Sung, *J. Photochem. Photobiol. A: Chemistry*, **171**, 269 (2005).
- [23] C. S. Chou, F. C. Chou, J. Y. Kang, *Powder Technology*, **215**, 38 (2012).
- [24] N. P. Ariyanto, H. Abdullah, *Funct. Mater. Lett.*, **3**, 303 (2010).

\*Corresponding author: huda@eng.ukm.my